

DIRECT NUMERICAL SIMULATION OF COMBINED EFFECTS OF WAKE AND DISCRETE SURFACE ROUGHNESS ON SEPARATED BOUNDARY LAYERS

Suleyman Karaca*
Istanbul Technical University
Istanbul, Turkey

Mark P. Simens†
Universidad Politécnica de Madrid
Madrid, Spain

Ayse G. Gungor‡
Istanbul Technical University
Istanbul, Turkey

ABSTRACT

The combined effects of unsteady large scale forcing and discrete surface roughness on the boundary layer development of a low-pressure-turbine like boundary layer is studied by direct numerical simulation using a high resolution numerical scheme. The results show a decrease in the extent of the separation bubble as well as the separation position compared with the baseline case without surface roughness and unsteady forcing. Furthermore, it is found that the effect of the roughness is negligible compared with the effect of wakes.

INTRODUCTION

The energy saving and the fuel emission are of great interest especially for civil and military aviation because of the increase in fuel prices and environmental reasons. Increasing the efficiency of the low-pressure-turbine (LPT) blade will reduce the fuel consumption and emissions. Boundary layer losses are the main reason for the decreasing efficiency. Experiments show that the dominant effect on the boundary layer loss is generated by the suction side of the LPT blade. During the service operation, LPT airfoils are exposed to different aerodynamic loadings. For instance, the aerodynamic loading of the LPT airfoils increases during take-off; that causes a growth of the adverse pressure gradient on the suction side, the boundary layer thickness grows and a laminar separation bubble size is formed and increases in size as well. The efficiency of the LPT blade will, therefore, decrease. To increase the blade efficiency, the laminar separation size must be controlled by active or passive flow control mechanisms [Montomoli et al., 2010].

LPT blades contain complex flow phenomena with unsteady separation due to the adverse pressure gradient (APG), reattachment, and wake interactions from the previous blade. These factors control the efficiency of the LPTs. The passive control mechanisms that are investigated in this study, are the wake passing frequency, the surface roughness and both. Effects of unsteady wakes on very high lift airfoils were investigated experimentally by [Volino, 2012; Hodson et al., 2005] and many other researchers. These studies show that in the case of low Reynolds number and very high-lift (aggressive) airfoils, without the wake effect, the boundary layer separates but does not reattach. Whereas this characteristic of the boundary layer changes when the wake effect is introduced. For the low wake passing frequency, the boundary layer separates between wakes then reattachment occurs. In the case of high wake passing frequency, the separation bubble size decreases significantly since there is not enough time between each wake passing for the separation bubble to regenerate itself. Overall, these experimental studies reported that the reattachment of the boundary layer is because of the wakes shed by the upstream rods. Another passive control mechanism of LPT is the surface roughness. The experimental studies that investigate the effect of roughness height, the location and the type indicate that the boundary layer development depends on these roughness parameters [Wörner et al., 2002]. Optimum values

*GRA, Faculty of Aeronautics and Astronautics, Email: karacasu@itu.edu.tr

†School of Aeronautics, Email: mark@torroja.dmt.upm.es

‡Assist.Prof., Faculty of Aeronautics and Astronautics, Email: ayse.gungor@itu.edu.tr

of these variables depend on the flow condition. Therefore, the operation range must be wide enough in the design of the passive control mechanisms. In the case of low Reynolds numbers and low free stream turbulence, the laminar separation bubble is suppressed substantially by the roughness effect [Lorenz et al., 2012]. [Zhang and Hodson, 2005] and [Montomoli et al., 2010] showed that at low Reynolds numbers, the wake passing frequency is not enough to suppress the large separation bubble. However, the laminar separation bubble size can be reduced more with using the roughness effect. The wake passing frequency and the roughness effects were mentioned separately before. Whereas their combined effects are of great interest as well, which is the focus of this study.

To understand the behaviour of the boundary layer development and the physics of the problem, we initiated a direct numerical simulation (DNS) study series. We begin with the investigation of the wake interactions [Gungor et al., 2012] and then, the roughness effects [Simens and Gungor, 2013] on the separated boundary layers. The wake interactions (wake passing frequency, shape factor and intensity) on the low pressure turbine blade are systematically examined by [Gungor et al., 2012]. It is concluded that the laminar separation and the turbulent transition are mainly effected by the wake passing frequency but the wake shape and intensity have little effect on the development of the boundary layer. Results indicate that the wake-passing frequency is the key parameter to control the separated region, and hence the turbine efficiency. Furthermore, in a recent study [Simens and Gungor, 2013], we showed the roughness effects on a laminar separation bubble, formed on a flat plate due to a strong adverse pressure gradient similar to those encountered on the suction side of typical low-pressure turbine blades. Results indicate that the laminar separation and turbulent transition are mainly affected by the type, the height and the location of the roughness element, and the separation bubble can be controlled by positioning the roughness element away from the separation bubble. Our previous studies that show the individual effect of wakes and roughness on low-pressure turbine type boundary layer flows revealed an important question. What will happen to the boundary layer development and hence the turbine efficiency when combining the effects of roughness and wakes?

The purpose of this research is to search for answers to this question, to gain fundamental understanding of laminar separation bubble behavior and some insight into their control, identify the key parameters for efficiency, and constitute a database for the academic and industrial studies. For this purpose, we investigate low-pressure-turbine like boundary layers subject to adverse-pressure-gradient, surface roughness and wakes using DNS approach.

This paper is organized as follows: after describing the numerical setup we discuss in detail the combined effect of wake passing frequency and discrete surface roughness on the separated flow. Important statistical quantities are shown and compared with the unforced flow. Finally, the paper ends with conclusions.

NUMERICAL SETUP

In this study, the low pressure turbine blade modelled as a flat plate with a pressure distribution similar to suction side of low pressure turbine blades. The flat plate model was validated experimentally on high-lift low-pressure turbine blade (T106C). Pressure distributions and boundary conditions are taken from [Zhang and Hodson, 2005]'s experiment. To model the LPT blade on a flat plate a nearly constant suction velocity was imposed at the upper boundary. Therefore, the pressure distribution along the flat plate is representative of those in LPTs.

The DNS code solves the incompressible Navier-Stokes equations with forth order compact spatial discretization for convective and viscous terms, third order Runge-Kutta scheme for time integration and second-order discretization for the pressure terms. Details concerning the numerical method can be found in [Simens et al., 2009; Simens, 2009]. The discrete roughness elements are modeled using the immersed boundary method [Fadlun et al., 2000; Uhlman, 2005]. The wakes are generated by the mean wake deficit created by a linear row of circular cylinders moving in the y-direction with a non dimensional passing frequency of $St = 1.55$, and superimposed at the inflow velocity profiles.

The Reynolds number based on the inflow momentum thickness $\theta_0 = 0.268$ mm and the free stream velocity $U_{ref} = 6.3$ m/s is $Re_{\theta_0} \approx 110$. The cost of DNS is highly related with the Reynolds number (for 3D domain $Re^{(9/4)}$), however, for our case the Reynolds number ($U_{ref} L_x / \nu = 170,000$) is low enough for an expensive DNS.

The streamwise, wall-normal and spanwise directions and velocity components are x, y, z and u, v, w, respectively. The simulation domain ($L_x \times L_y \times L_z$)/ $\theta_0 = 1640 \times 468 \times 123$ is discretized in $N_x \times N_y \times N_z = 1537 \times 301 \times 768$ collocation points and there are approximately 330 million grid points. All flow structures in the spatial and temporal space are resolved properly from the smallest scale (Kolmogorov scale) to the largest scale (integral scale). The grid resolution at the wall is $\Delta y^+ \approx 0.4$, towards to boundary layer $\Delta y^+ \approx 2$ while

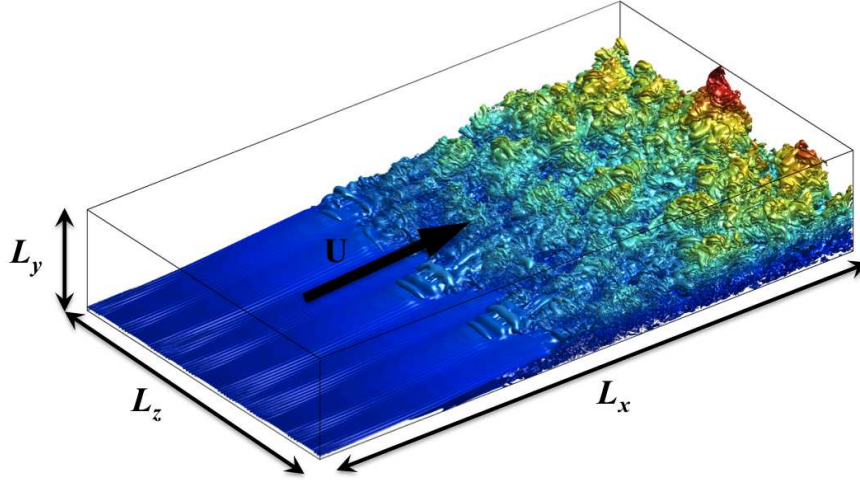


Figure 1: The numerical setup and the instantaneous visualization of the spanwise vorticity in an adverse pressure gradient turbulent boundary layer. The vortices are coloured with the distance to the wall; blue (dark) near the wall, and red near the top. Flow is from bottom-left to top-right.

Table 1: Parameters of the adverse-pressure-gradient boundary layer simulations. The case $\mathcal{RW}0$ is a base uncontrolled simulation by [Simens et al., 2009], used for comparison. The wake parameter $St = \frac{fL_x}{U_{ref}}$, is the Strouhal number based on the wake passing frequency, the length of the plate and the reference velocity at the inlet. The roughness parameters, h_r , x_r and k_r are the height, location and wavenumber, respectively. The pressure gradient parameter at separation point, $\Lambda_s = \frac{\theta_s^2}{\nu} \frac{dU_\infty}{dx}|_s$, lies in the range $-0.171 < \Lambda_s < -0.083$ as suggested in [Thwaites, 1949] for laminar separation. L_b/L_{b0} is the ratio of the length of the separated region to length of the unforced separation region. The momentum thickness, θ_0 is measured at the inflow.

Case	St	$k_r\theta_0$	h_r/θ_0	x_r/θ_0	Re_θ	Λ_s	L_b/L_{b0}
$\mathcal{RW}0$	0	0	0	0	110-1600	-0.089	1.0
$\mathcal{R}3d$	0	0.008	0.70	50	110-1022	-0.11	0.512
$\mathcal{W}St155$	1.55	0	0	0	110-980	-0.118	0.3810
$\mathcal{R}3d\mathcal{W}St1.55$	1.55	0.008	0.70	50	110-895	-0.1168	0.3619

$\Delta x^+ \approx \Delta z^+ \approx 2$ [Gungor et al., 2012]. No-slip boundary conditions are applied on the wall and the spanwise direction is treated as periodic. At the outflow plane a convective boundary condition is used, with a minor adjustment to the exit velocity to ensure global mass conservation [Gungor et al., 2012].

The integration domain along with the instantaneous vorticity contours is shown in Fig. 1. As seen from the figure this type of flow contains complex phenomena with unsteady separation, reattachment, wakes, and vortex interactions. Table 1 summarizes the parameters used for the various simulations presented here.

A variable time interval is used, determined by a constant $CFL = 0.6$ condition. The time interval is approximately $10.6 \mu s$. So, even though the domain is small, the computations are intense. For example, the computational time for one wake passing is 7K CPU hours. The velocity field evolved for about 10 wake passing periods for the initial washout, and statistics are collected for another 10 periods, with a total cost of 140K CPU hours.

RESULTS

Statistics of the velocity are compiled over 10 wake passing periods for the $\mathcal{R}3d\mathcal{W}St1.55$ case. Figure 2 presents the instantaneous streamwise velocity fluctuations for the separate and combined effects of surface trip and wake passing. The uncontrolled flow is initially laminar, separates, transitions within the separation bubble, reattaches due to the transition, and develops into an attached turbulent APG boundary layer. The distributed surface roughness increases the turbulent fluctuations in the turbulent boundary layer and it shifts the laminar-turbulent transition at some upstream position, as shown in Fig 2b. The forcing, in which all the turbulent fluctuations except for the mean velocity defect are neglected, triggers the transition of the separated

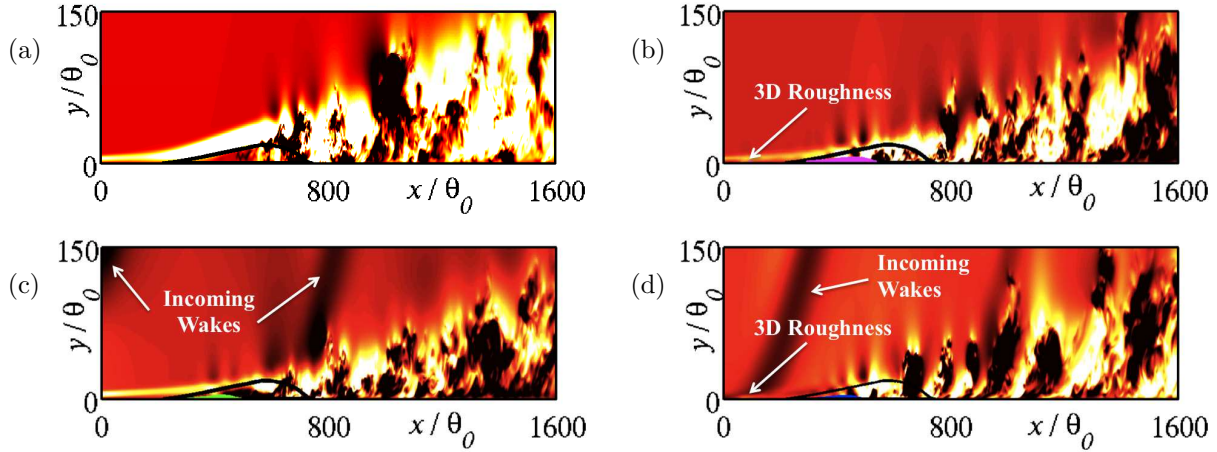


Figure 2: Streamwise velocity fluctuation (shaded contours) and the zero contour of the streamwise velocity (lines). The contours are $(-0.05, 0.1)$ of the reference velocity. (a) $\mathcal{RW}0$; (b) 3D roughness, $\mathcal{R}3d$; (c) Wake, $\mathcal{W}St1.55$; (d) 3D roughness and wakes, $\mathcal{R}3d\mathcal{W}St1.55$.

shear layer, modifies the separated region, and results in a shorter and lower separation bubble (Fig. 2c). The combined effect exerts different effects at the flow. Both effects decrease the boundary layer losses and hence the drag forces by reducing the separation length and height of the laminar bubble.

Figures 3 and 4 show the development of the mean flow properties of the rough and wake simulation as a function of the streamwise location, x/θ_0 . It is compared with the APG simulation in [Simens et al., 2009], the wake simulation in [Gungor et al., 2012], and the three-dimensional roughness simulation in [Simens and Gungor, 2013]. In the unperturbed case, a large unsteady separation bubble due to the adverse pressure gradient exist. Momentum thickness describes the momentum deficit in the boundary layer. Figure 3 shows the momentum thickness (normalised by the inflow momentum thickness) as a function of streamwise direction. It is clear in this figure that in the uncontrolled flow the momentum deficit is high compared to $\mathcal{R}3d$, $\mathcal{W}St1.55$, $\mathcal{R}3d\mathcal{W}St1.55$ cases. So, the efficiency of the momentum transfer is high in the flow controlled cases by the reason of increasing wall-normal mixing and due to accelerated flow of the roughness element as mentioned previous paragraph. These effects causes high momentum transfer rate.

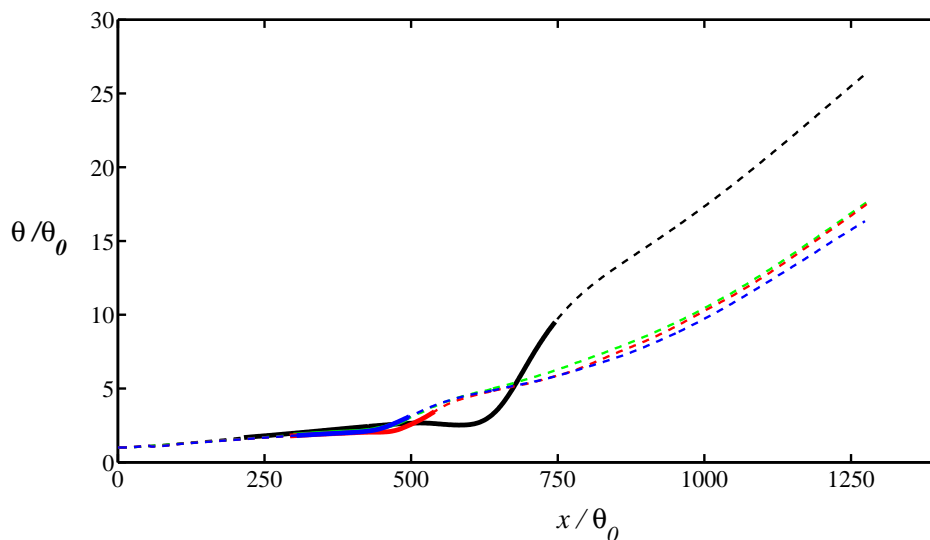


Figure 3: Streamwise momentum thickness normalised by inflow momentum thickness. Black: $\mathcal{RW}0$, Red: $\mathcal{R}3d$, Green: $\mathcal{W}St1.55$, Blue: $\mathcal{R}3d\mathcal{W}St1.55$. — : separated flow, $C_f < 0$, and ---- : attached flow, $C_f > 0$.

The individual and combined effects of discrete surface roughness and wakes can be seen on both ends of

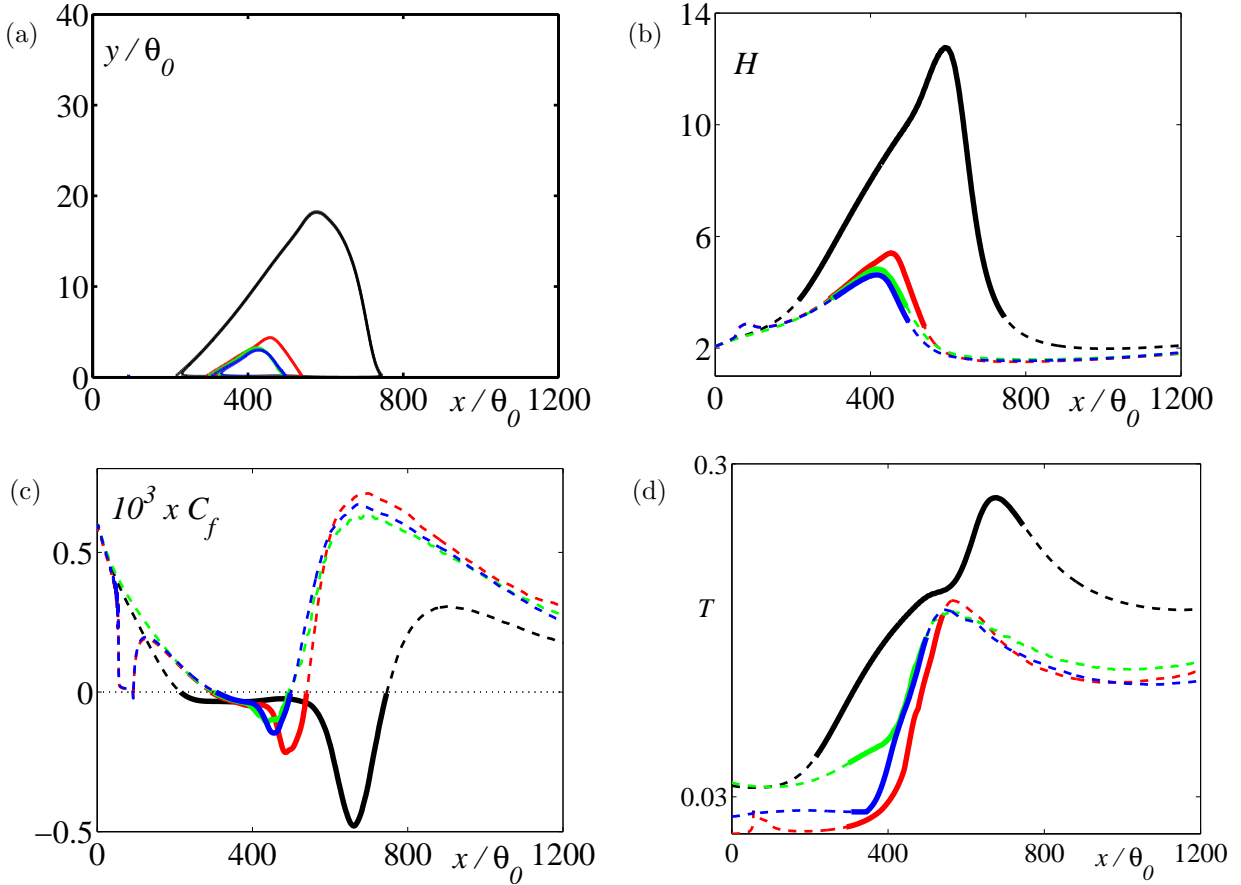


Figure 4: The separated and combined effects of surface trip and wake passing on the mean flow statistics. (a) Zero contour of the streamwise velocity, indicates the location of the separation bubble; (b) Shape factor; (c) Skin friction coefficient; (d) Maximum turbulent intensity. Black: $\mathcal{RW}0$, Red: $\mathcal{R}3d$, Green: $\mathcal{W}St1.55$, Blue: $\mathcal{R}3d\mathcal{W}St1.55$. — : separated flow, $C_f < 0$, and ---- : attached flow, $C_f > 0$.

the bubble, as shown in Fig. 4a. Not only the reattachment point moves upstream but also the separation point moves downstream, while the height of the separation bubble is reduced. This is due to a mean flow deformation by the wake transport of mean momentum towards the near-wall region in the case of the large-scale wake forcing, and due to accelerated flow in the openings of the three-dimensional roughness element. The separate and combined effects of surface trip and wake passing on the time averaged shape factor $H = \delta^*/\theta$ and the skin friction coefficient $C_f = \tau_w / \frac{1}{2} \rho U_{ref}^2$ (with $\tau_w = \mu d\langle U \rangle / dy|_{y=0}$) are compared in Figs. 4b and c, respectively. It can be seen that the unperturbed case results in a longer region of separated flow with a flat skin friction distribution and higher values of the shape factor. The large-scale forcing and roughness alter the boundary layer development, resulting in a significant decrease in the overall displacement of the separation bubble and length. The streamwise variation of the maximum turbulent intensity, $T(x) = \max_y \left(\sqrt{\frac{1}{3} (\overline{u'u'} + \overline{v'v'} + \overline{w'w'})} / U_\infty(x) \right)$ is shown in Fig. 4d. For the controlled cases, the growth of the disturbances in the initial part of the separated region is slow, whereas they grow much faster in the downstream part of the separated region. This sudden growth of the streamwise fluctuations triggers a slowdown of bubble growth due to turbulent energy diffusion and is responsible for the increase in the skin friction.

The turbulent kinetic energy contours shown in Fig. 5 provides a clear view of the turbulent activity around the separated region. The time-averaged separation region and the boundary layer thickness development are also indicated in the same plot with thick solid lines. The symbols shown indicate the inflection points in the velocity profile. The profiles have an inflection point imposed by the APG, which is the precursor of the boundary layer separation. Flow fluctuations originate on the line of inflection points in the velocity profile. The line of inflection points is significant for the development of transition and reattachment. with boundary layer thickness. The wakes and roughness elements give the flow, initially two-dimensional perturbations. Individual studies on the effect of roughness and wakes show that both modifies the spatial development of

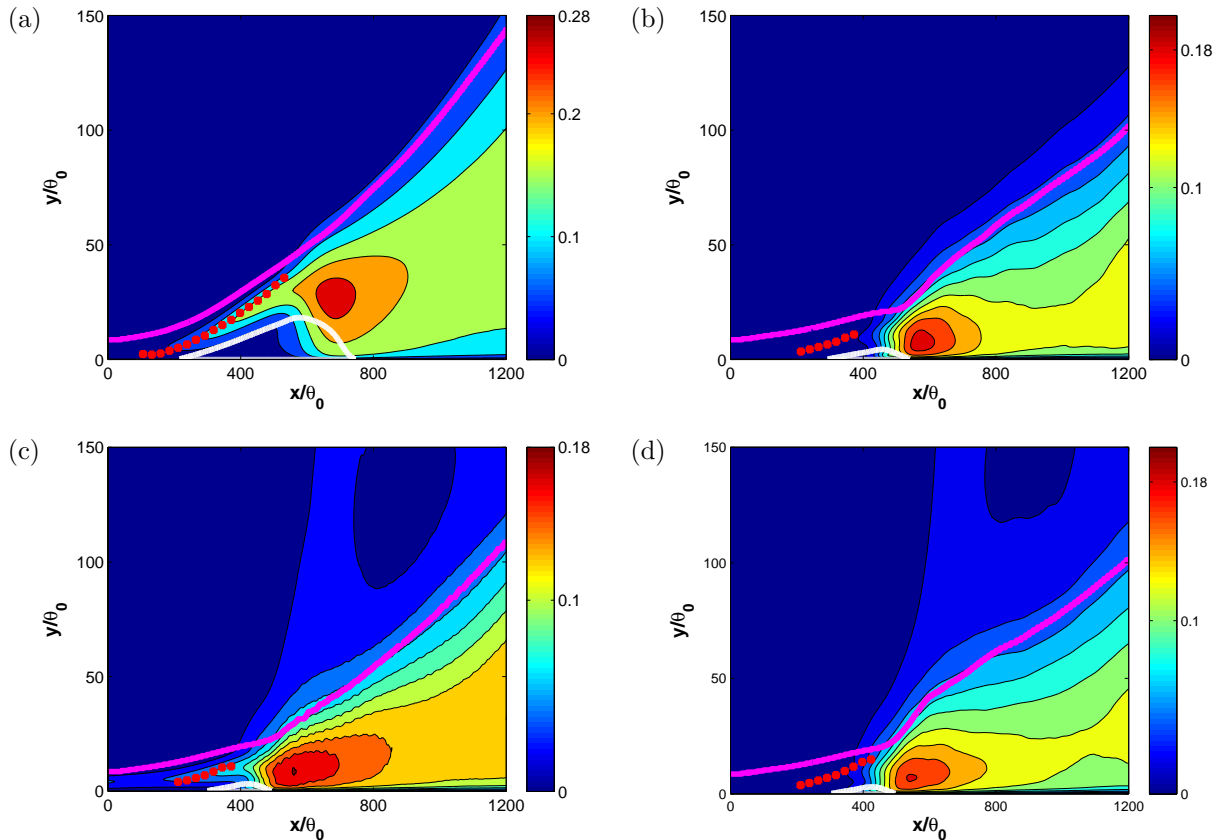


Figure 5: Turbulent kinetic energy contours (shaded contours), the boundary layer thickness (magenta lines), inflectional points (red symbols) and the zero contour of the streamwise velocity (white lines). The contours are nondimensionalized by the reference velocity. (a) $\mathcal{RW}0$; (b) 3D roughness, $\mathcal{R}3d$; (c) Wake, $\mathcal{W}St1.55$; (d) 3D roughness and wakes, $\mathcal{R}3d\mathcal{W}St1.55$.

the laminar boundary layer by promoting the transition. And their combined effect is clearly seen in Fig. 5 from the boundary layer thickness lines and Fig. 4d (see the peak points of maximum turbulent kinetic energy figure). This is because the flow is still laminar. In the region of transition the perturbations become three-dimensional. By the reason of these effects, in Fig. 5(a to d) maximum kinetic energy level and boundary layer development move close to the wall.

CONCLUSION

We investigate the low-pressure-turbine like boundary layers subject to adverse-pressure-gradient, surface roughness and wakes using DNS approach. Results indicate that the laminar separation and turbulent transition are mainly affected by the combined effects of large-scale forcing and discrete roughness. The separation bubble can be controlled by positioning the roughness element away from the separation bubble and introducing the large scale wake forcing. The effect of the boundary layer trip is negligible compared to the wake effect. As a result, the mean flow statistics show almost similar trends for the unsteady smooth and rough cases. Further work will extend these studies to lower wake passing frequencies, and focus on optimizing the large-scale based control.

ACKNOWLEDGMENT

The computations were made possible by generous grants of computer time from the Barcelona Supercomputing Centre (BSc) and from the National Center for High Performance Computing of Turkey (UYBHM) under grant number 1002222012.

References

- Fadlun, E.A., Verzicco, R., Orlandi, P., and Mohd-Yusof, J. (2000) *Combined immersed-boundary finite-difference methods for three-dimensional complex flow simulations*, J. Comp. Physics, Vol. 161, pp:35-60.
- Gungor, A.G., Simens, M.P., Jimenez, J. (2012) *Direct numerical simulations of wake-perturbed separated boundary layers*, ASME J. Turbomach., Vol. 134, pp:1-9.
- Hodson, H.P., and Howell, R.J. (2005) *Bladerow interactions, transition and high-lift aerofoils in low-pressure turbine* Annu. Rev. Fluid Mech., Vol. 37.
- Lorenz, M., Schulz, A. and J. Bauer, H. (2012) *Experimental study of surface roughness effects on a turbine airfoil in a linear cascade-Part II: Aerodynamic losses* ASME J. Turbomach., Vol. 134, pp:1-11.
- Montomoli, F., Hodson, H. and Haselbach, F. (2010) *Effect of roughness and unsteadiness on the performance of a new low pressure turbine blade at low Reynolds numbers*, ASME J. Turbomach., Vol. 132, pp:1-9.
- Simens, M.P., Jimenez, J., Hoyas, S., and Mizuno, Y. (2009) *A high-resolution code for turbulent boundary layers*, J. Comput. Phys., Vol. 228, pp. 4218-4231. Facebook
- Simens, M.P. (2009) *The study and control of wall bounded flows*, Ph.D. Thesis, Universidad Politecnica de Madrid, Spain.
- Simens, M.P. and Gungor, A.G. (2013) *Effect of surface roughness on laminar separated boundary layers*, Proceedings of ASME Turbo Expo 2013.
- Thwaites, B. (1949) *Approximate calculation of the laminar boundary layer*, Aero. Q., Vol. 1, pp:61-85.
- Uhlmann, M. (2005) *An immersed boundary method with direct forcing for the simulation of particulate flow*, J. Comp. Physics, Vol. 209, pp:448-476.
- Vera, M., Hodson, H.P., Vazquez, R., 2005, *The effects of a trip wire and unsteadiness on a high-speed highly loaded low-pressure turbine blade* ASME J. Turbomach., Vol. 127, pp:747-754.
- Volino, R.J. (2012) *Effect of unsteady wakes on boundary layer separation on a very high lift low pressure turbine airfoil*, ASME J. Turbomach., Vol. 134.
- Wörner, A., Rist, U., and Wagner, S. (2002) *Influence of humps and steps on the stability characteristics of a 2D laminar boundary layer*, AIAA 2002-0139.
- Zhang, X.F. and Hodson, H. (2005) *Combined effects of surface trips and unsteady wakes on the boundary layer development of an ultra-high-lift turbine blade*, ASME J. Turbomach., Vol. 127, pp:479-488.